

DAMAGE AND FRACTURE ANALYSIS OF BOLTED JOINTS OF COMPOSITE MATERIALS BASED ON PERIDYNAMIC THEORY

Na-Na Yang

Tian-You Zhao

Ji-Guang Gu

Zhi-Peng Chen

Harbin Engineering University, China

ABSTRACT

It is clear that the advantages of fibre glass-reinforced plastics surpass those of steel, but the failure analysis of composite structures is much more complex than that of isotropic materials as composite materials may fail in a variety of ways. In order to simulate the damage and fracture of bolted joints of fibre reinforced composite, the bond-based peridynamic method suitable for elastic, brittle and anisotropic characteristics of composite material is used. The peridynamic model for composite laminate is validated by the finite element method. Then a peridynamic program of composite damage is applied to calculating the damage of bolted joint structure and the damage propagation process and failure mode of the structure is obtained.

Keywords: Peridynamic theory, composite material, damage and fracture, joints

INTRODUCTION

Composite materials have been widely used in modern engineering due to their high ratios of strength and stiffness to weight. It is clear that the advantages of fibre glass-reinforced plastics surpass those of steel, but the failure analysis of composite structures is much more complex than that of isotropic materials as composite laminates may fail in a variety of ways. At present, there are many theoretical and numerical methods to simulate the damage and fracture of composites, the most widely used of which is the classic theory of continuum mechanics. However, it can be rather challenging to solve this way the discontinuity problems such as structural damage, crack propagation, delamination and penetration. The motion equations in classic continuum mechanics are in the form of partial differential equations, that involve the spatial displacement derivatives, but these derivatives are undefined when the displacement are discontinuous. It is difficult to simulate the process of crack generation and propagation, even though with the aid of dynamic grid or adaptive grid technology.

Researchers put forward the cohesive elements [1] and Extended Finite Element Method (XFEM) [2] to introduce the additional function reflecting the discontinuity in the finite element method, but there is still a great challenge for complex damage of composite.

In 2000, Silling proposed a non-local particle method, named Peridynamics (PD) [3], shown in Fig. 1, which combines the advantages of molecular dynamics, meshless method and finite element method [4]. In PD theory, the solution domain is discretized into a finite number of material points, the interaction between different material points is used to describe the non-local interaction between particles and the state of a material point is influenced by the number of points located in a region of defined radius. The main difference between the PD and classic continuum mechanics is the using of integral equations instead of derivatives of the displacement components, therefore such approach is especially suitable to predict the damage and fracture process of composite materials. Moreover, in the PD theory internal forces are expressed through non-local interactions between pairs of material points within

a continuous body and damage is a part of the constitutive model. This feature allows to model damage initiation and propagation at multiple region with arbitrary paths inside the material without resorting to special crack growth criteria.

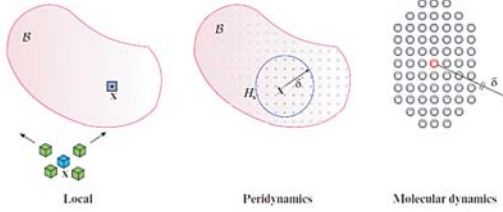


Fig. 1. Local and non-local continuum models [5]

PERIDYNAMIC THEORY OF COMPOSITE LAMINATES

The fibre reinforced composite plate of structure shown in Fig. 2 is analyzed in this paper. Laminated plate is a structure composed of a certain number of lamina according to the corresponding rules. The so-called fibre orientation in composite structure is the angle between a fibre and x coordinate axis and each lamina has its own properties and thickness. For the orthotropic lamina there are four independent material constants, namely: the elastic modulus in longitudinal direction E_{11} , elastic modulus in transverse direction E_{22} , in-plane shear modulus G_{12} , and in-plane Poisson's ratio ν_{12} .

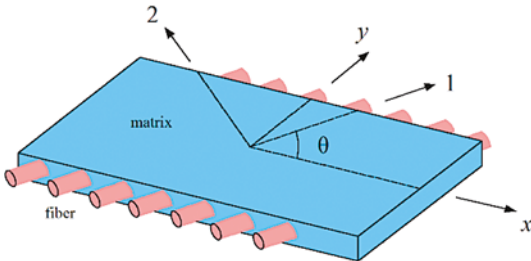


Fig. 2. A lamina and its material coordinate system

Composite materials have the characteristics of inhomogeneity and anisotropy compared with isotropic materials, therefore different kinds of bonds are usually needed to describe them. For the bond-based peridynamic model of fibre reinforced composite laminates, fibre bonds, matrix bonds, interlayer bonds and shear bonds are defined to describe the in-plane, interlayer and shear characteristics [6], that is to say there are matrix bonds between the material points in each ply, the fibre bonds exist only between the material points along the direction of layer angle, the interlayer bonds exist only in the material points in the vertical direction of the adjacent layer, while the shear bonds exist in the other direction of the adjacent layer. The model diagram is shown in Fig. 3. Each bond constant can be obtained by equating the strain energy density expressed by peridynamics and the classic continuum mechanics for a composite under simple loading.

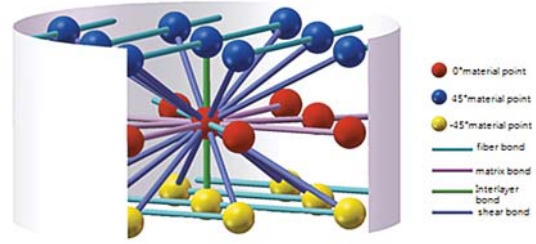


Fig. 3. Bond-based peridynamic model of fibre reinforced composites[6]

For the lamina, the thickness is usually far smaller dimension than that in other direction, therefore it can be approximately assumed that $\sigma_3 = 0, \tau_{23} = \tau_{13} = 0$. For orthotropic materials in plane stress state the stress-strain relationship can be expressed as:

$$\begin{Bmatrix} \sigma_{11} \\ \sigma_{22} \\ \tau_{12} \end{Bmatrix} = \begin{bmatrix} Q_{11} & Q_{12} & 0 \\ Q_{12} & Q_{22} & 0 \\ 0 & 0 & Q_{66} \end{bmatrix} \begin{Bmatrix} \varepsilon_{11} \\ \varepsilon_{22} \\ \gamma_{12} \end{Bmatrix} \Rightarrow \boldsymbol{\sigma} = \mathbf{D}\boldsymbol{\varepsilon} \quad (1)$$

where \mathbf{D} is the stiffness matrix of the material, each component of which is represented as: $Q_{11} = E_{11}/(1 - \nu_{12}\nu_{21})$, $Q_{66} = G_{12}$, $Q_{22} = E_{22}/(1 - \nu_{12}\nu_{21})$, $Q_{12} = \nu_{21}E_{22}/(1 - \nu_{12}\nu_{21})$. When the layer angle between the principal direction of the fibre and X-axis is θ , the stress-strain relationship of the lamina is as follows:

$$\begin{Bmatrix} \sigma_x \\ \sigma_y \\ \tau_{xy} \end{Bmatrix} = \begin{bmatrix} \bar{Q}_{11} & \bar{Q}_{12} & \bar{Q}_{16} \\ \bar{Q}_{12} & \bar{Q}_{22} & \bar{Q}_{26} \\ \bar{Q}_{16} & \bar{Q}_{26} & \bar{Q}_{66} \end{bmatrix} \begin{Bmatrix} \varepsilon_x \\ \varepsilon_y \\ \gamma_{xy} \end{Bmatrix} = \bar{\mathbf{Q}} \begin{Bmatrix} \varepsilon_x \\ \varepsilon_y \\ \gamma_{xy} \end{Bmatrix} \quad (2)$$

where $\bar{\mathbf{Q}}$ is the reduced stiffness matrix of the material.

In the classic continuum mechanics, the strain energy density W^{CM} at any point of two-dimensional composite lamina can be expressed as:

$$W^{CM} = \frac{1}{2} \boldsymbol{\sigma}^T \boldsymbol{\varepsilon} = \frac{1}{2} \sigma_{11} \varepsilon_{11} + \frac{1}{2} \sigma_{22} \varepsilon_{22} + \frac{1}{2} \sigma_{12} \gamma_{12} \quad (3)$$

or

$$W^{CM} = \frac{1}{2} (Q_{11} \varepsilon_{11}^2 + 2Q_{12} \varepsilon_{22} \varepsilon_{11} + Q_{66} \gamma_{12}^2 + Q_{22} \varepsilon_{22}^2) \quad (4)$$

In the PD theory the strain energy density at arbitrary material point can be obtained by integrating the micro-potential energy of the material points in the defined horizon. The strain energy density of the material point k can be expressed as:

$$W^{PD} = \frac{1}{2} \sum_{j=1}^N w_{(j)(k)} V_{(j)} + \frac{1}{2} \int_H w dH \quad (5)$$

where N indicates the number of fibre bonds in the horizon of the material point k , and the potential energy can be expressed according to the PD theory as:

$$w = \frac{1}{2} c(\phi) s^2(\phi) \xi \quad (6)$$

It is worth noting that the stretch of bonds between material point k and j , $s(\phi)$, is expressed in the polar coordinate system,

as shown in Fig. 4. The bond constant $c(\phi)$ in the PD theory can be expressed as:

$$c(\phi) = \begin{cases} c_F + c_A & \phi = \theta \\ c_A & \phi \neq \theta \end{cases} \quad (7)$$

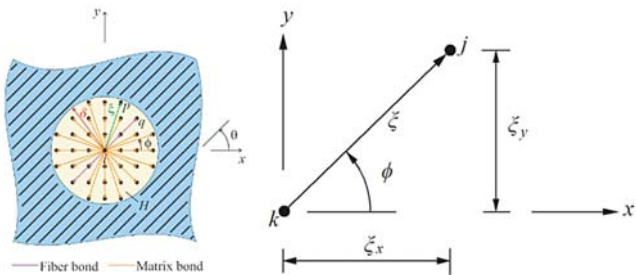


Fig. 4. Stretch of material points k in PD model of lamina [7]

Therefore, W^{PD} can be expressed by substituting Eqs. (6)~(7) into (5):

$$W^{PD} = \frac{1}{2} \sum_{j=1}^N \frac{c_F s_{jk}^2 \xi_{jk}}{2} V_{(j)} + \frac{1}{2} \int_H \frac{c_A s^2 \xi}{2} dH \quad (8)$$

Putting $W^{PD} = W^{CM}$, the bond constants of fibre and matrix under action of shear, axial tension and other loads can be expressed as:

$$c_F = \frac{2E_{11}(E_{11} - E_{22})}{(E_{11} - \frac{1}{9}E_{22})(\sum_{j=1}^N \xi_{jk} V_{(j)})} \quad (9)$$

$$c_A = \frac{8E_{11}E_{22}}{(E_{11} - \frac{1}{9}E_{22})\pi t \delta^3} \quad (10)$$

It is assumed that the relative displacement occurs between a material point a and other material points in the horizon within the laminate, as shown in Fig. 5, the strain energy density at the material point a can be expressed by the sum of the strain energy density of interlayer bond and shear bond.

$$W^{PD} = \hat{W}^{PD} + \tilde{W}^{PD} = \frac{1}{2} \sum_{j=d,e} \frac{c_N s_{ja}^2 \xi_{ja}}{2} V_j + \frac{1}{2} \int_H \frac{c_S \varphi^2}{2} dH \quad (11)$$

where the shear angle φ can be obtained by averaging the shear angle φ_{ad} between the material point a, d and the shear angle φ_{bc} between the material point b and c , as shown in Fig. 6.

$$\varphi = \frac{\varphi_{da} + \varphi_{bc}}{2} \quad (12)$$

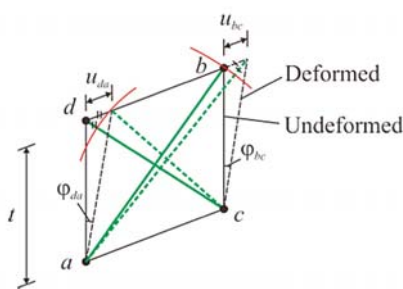


Fig. 5. Definition of shear angle [7]

As shown in Fig. 6, the interlayer bond and shear bond can be obtained by equating the strain energy density expressed by the PD theory and the continuum mechanics. It is worth noting that the strain energy density due to the deformation is related to the matrix material parameters which are independent of the fibre material parameters.

$$c_N = \frac{E_m}{t\bar{V}}, \quad c_S = \frac{2G_m}{\pi t} \frac{1}{\delta^2 + t^2 \ln(t^2 / (\delta^2 + t^2))} \quad (13)$$

where, \bar{V} is the volume of the material point d and e , $\bar{V} = V_d = V_e$. t is the interlayer thickness, E_m and G_m are the elastic modulus and the shear modulus of matrix material, respectively. For the material points near the free surface, the surface correction is required because the material points are there not entirely embedded within its horizon.

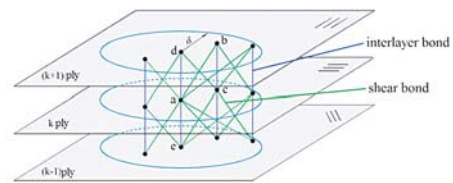


Fig. 6. The interlayer and shear bond of the laminates [7]

The damage can be determined by using the strength of macroscopic materials [8]: the critical stretch of the fibre and matrix bond are: $s_{ff} = X_T/E_{11}$ ($s \geq 0$) and $s_{mt} = Y_T/E_{22}$ ($s \geq 0$), respectively. The critical compression of the fibre and matrix bond are: $s_{fc} = X_C/E_{11}$ ($s < 0$) and $s_{mc} = s_{fc} = X_C/E_{11}$ ($s < 0$), respectively. The relationship between stretch and pair-wise response function is shown in Fig. 7.

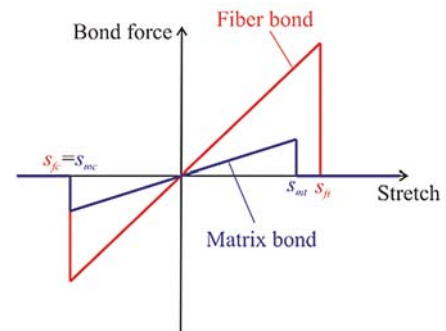


Fig. 7. Force-stretch relation for fibre and matrix bonds [8]

Oterkus and Madenci [5] proposed that the critical parameters of interlayer bond and shear bond based on the theory of fracture mechanics can be expressed as:

$$s_N = \sqrt{\frac{2G_{IC}}{tE_m}}, \quad \varphi_S = \sqrt{\frac{G_{IIC}}{tG_m}} \quad (14)$$

where G_{IC} and G_{IIC} are the mode-I and mode-II of critical energy release rate of the matrix material, respectively. It is worth noting that the interlayer bonds show only stretch failure of delamination as this is the main failure mode of laminates.

The relationship between the relative deformation and the force density function of the material points is shown in Fig. 8.

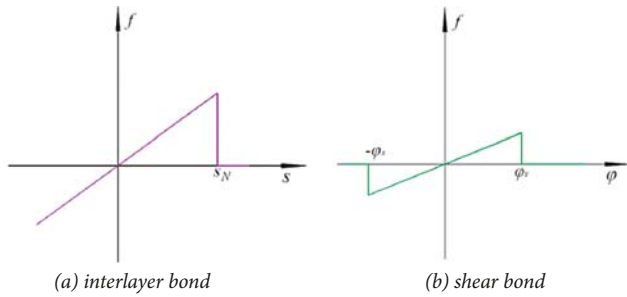


Fig. 8. The relationship between stretch of interlayer bond, shear angle and pair-wise response function

VALIDATION STUDY

In this section, a set of peridynamic calculation programs for composite structures is compiled based on the FORTRAN (2013) language and the Visual Studio (2012) environment and then used to simulate behaviour of two examples. Their results are compared with the simulation results obtained from the finite element software ABAQUS for checking validity of the composite PD models.

LAMINA WITH CIRCULAR HOLE

The finite element method and PD one are used to calculate the composite lamina with circular hole under axial tensile load. The particulars of the lamina shown in Fig. 9 are as follows: the thickness of 0.165 mm, the ply direction of 0° and

the axial tensile load of 159.96MPa. The material parameters are shown in Tab. 1. In the PD model there are 250 material points in the length direction, 75 material points in the width direction and the horizon radius is $\delta = 3\Delta x$. The displacement components in x- and y-directions calculated by using the finite element method and PD one are shown in Fig. 10. The horizontal and vertical displacements along the central axis are shown in Fig. 11. The results obtained from the finite element method and PD one are in a good agreement.

Tab. 1. The material parameters of the lamina

Elastic modulus in longitudinal direction	$E_{11} = 259.96$ GPa
Elastic modulus in transverse direction	$E_{22} = 8.96$ GPa
In-plane shear modulus	$G_{11} = 3.05$ GPa
In-plane Poisson ratio	$\nu_{12} = 1/3$
Density	$\rho = 1800$ kg/m ³

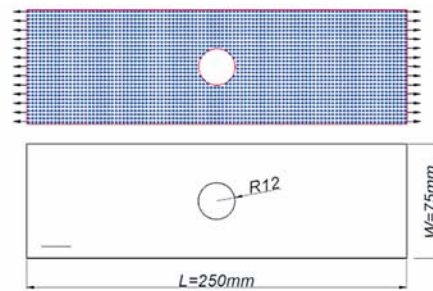


Fig. 9. PD model of the lamina with central circular hole

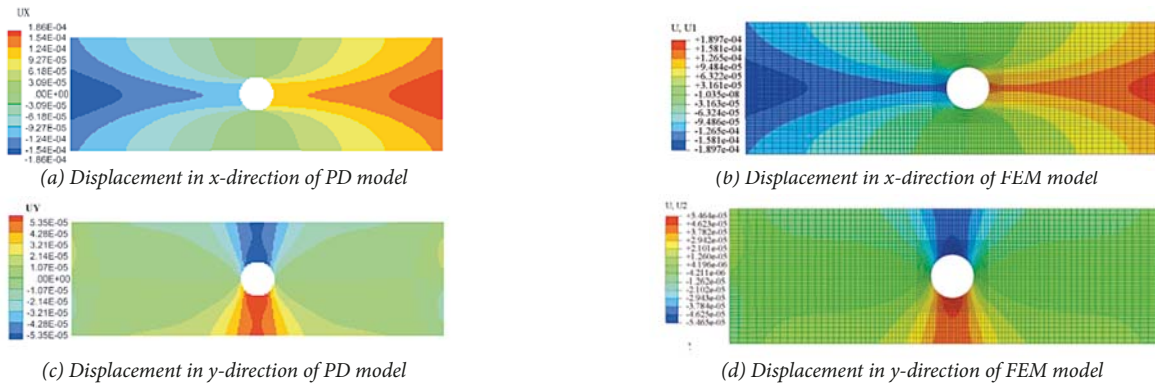


Fig. 10. Calculation results of displacements in PD and FEM models

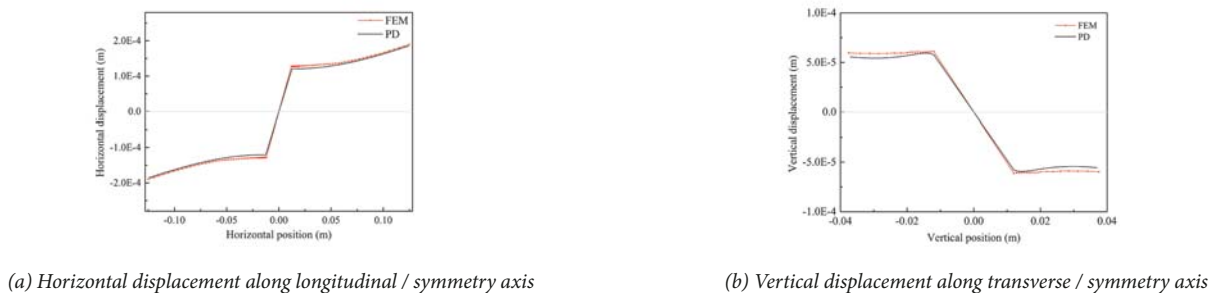


Fig. 11. Displacements along the symmetry axes in case of PD and FEM models

In the bond-based peridynamic models the stress results cannot be directly obtained. Therefore, in this paper the least square method is introduced to get the stress results from PD calculation process. The accuracy of the stress obtained from this method is significantly higher than that from the direct difference method. It is suitable for finding the solution of uniform discrete mesh-less space deviation. It is assumed that the displacement function at a material point is as follows:

$$\begin{cases} u(x, y) = a_0 + a_1x + a_2y \\ v(x, y) = b_0 + b_1x + b_2y \end{cases} \quad (15)$$

where a_0, a_1, a_2 and b_0, b_1, b_2 are polynomial coefficients to be fitted. The displacement matrix, location of material point k and other material points in the horizon are expressed in the form of matrix equation:

$$\begin{bmatrix} 1 & x_k & y_k \\ 1 & x_1 & y_2 \\ \dots & \dots & \dots \\ 1 & x_{n-1} & y_{n-1} \\ 1 & x_n & y_n \end{bmatrix} \begin{bmatrix} a_0 \\ a_1 \\ a_2 \end{bmatrix} = \begin{bmatrix} u_k \\ u_1 \\ \dots \\ u_{n-1} \\ u_n \end{bmatrix} \Rightarrow \mathbf{X}\mathbf{a} = \mathbf{u} \quad \forall |\mathbf{x}_n - \mathbf{x}_k| \leq \delta \quad (16)$$

The least squares method can be used to solve the undetermined coefficient matrix.

$$\mathbf{a} = \begin{bmatrix} a_0 \\ a_1 \\ a_2 \end{bmatrix} = (\mathbf{X}^T \mathbf{X})^{-1} \mathbf{X}^T \mathbf{u} \quad (17)$$

The displacement $v(x, y)$ can be obtained by the same way as well. The strain components at material points are given as follows:

$$\begin{aligned} \varepsilon_x &= \partial u / \partial x = a_1 \\ \varepsilon_y &= \partial v / \partial y = b_2 \\ \gamma_{xy} &= \partial u / \partial y + \partial v / \partial x = a_2 + b_1 \end{aligned} \quad (18)$$

The stress-strain relationship at the state of plane stress can be obtained by the equation (2). By comparing the stress results calculated with the use of PD and FEM methods, shown in Fig. 12, it is found that the two results are in good agreement.

LAMINA WITH PREFABRICATED CRACKS

The damage and fracture modes of laminas with central prefabricated cracks were analyzed and the effects of the central pre-crack angles on forms of in-plane damage and crack propagation were investigated. The lamina in question is 150 mm long, 50 mm wide and 0.165 mm thick, the central pre-crack length is 12 mm and the angle between x axis is set to be, successively: $-60^\circ, -45^\circ, -30^\circ, 0^\circ, 30^\circ, 45^\circ, 60^\circ$ and 90° . The assumed calculation model is shown in Fig. 13, the material point spacing in PD model $\Delta x = 0.625$ mm, the horizon radius $\delta = 3\Delta x$, the critical elongation of the resin bond is 0.0135, and the critical elongation of the fibre bond is 0.027. Simultaneously there is assumed: the tensile load speed $v = 8$ m/s in the plate width direction, the calculation time step equal to 2×10^{-8} s and the total number of steps reaching 5000.

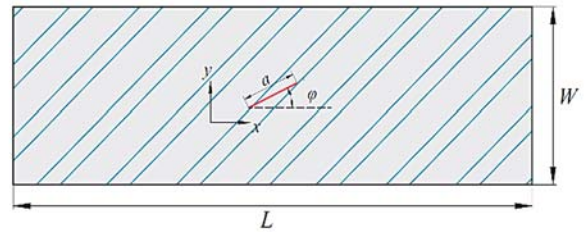


Fig. 13. The lamina with pre-crack under 45° angle

The results given below in Fig. 14 show that the damage mode of the lamina with pre-crack in its centre is mainly based on the tensile damage of the matrix, the direction of damage and crack propagation is always along the fibre

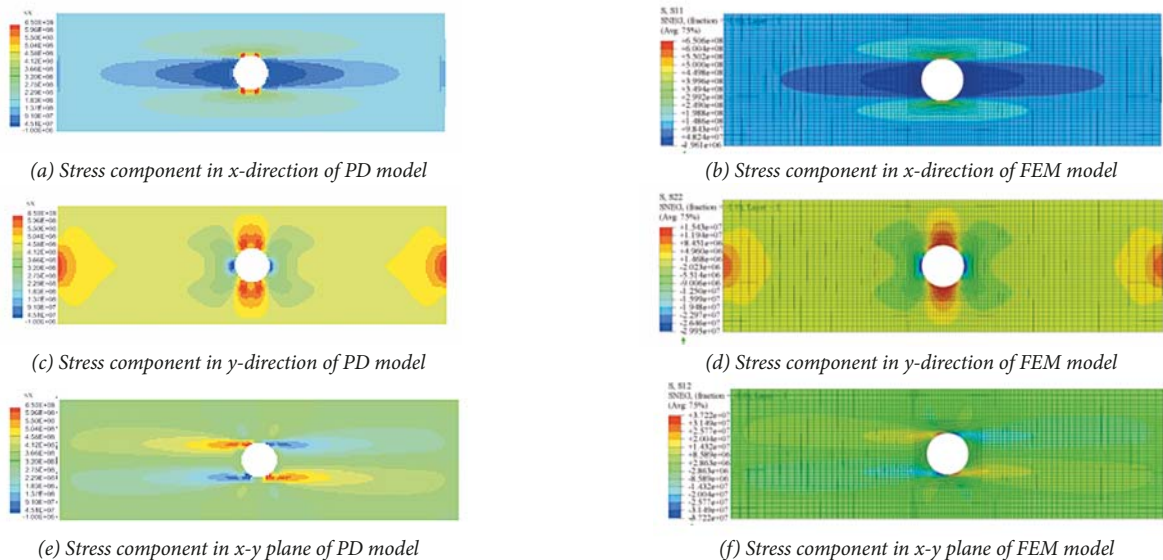


Fig. 12. Stress components in the lamina with central circular hole

DAMM: 0.05 0.15 0.25 0.35 0.45 0.55 0.65 0.75 0.85 0.95

UX: 4.5E-01 4.0E-01 3.25E-01 2.4E-01 2.0E-01 1.5E-01 1.25E-01 1.0E-01 5.2E-01



(a) -60° damage process



(b) -60° damage form of pre-crack



(c) -45° damage process



(d) -45° damage form of pre-crack



(e) -30° - damage process



(f) -30° - damage form of pre-crack



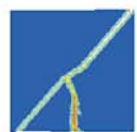
(g) 0° - damage process



(h) 0° - damage form of pre-crack



(i) 30° - damage process



(j) 30° - damage form of pre-crack



(k) 45° - damage process



(l) 45° - damage form of pre-crack



(m) 60° - damage process



(n) 60° - damage form of pre-crack



(o) 90° - damage process



(p) 90° - damage form of pre-crack

Fig. 14. Pre-crack damage and crack propagation for different pre-crack angles

direction and the damage starts from the tip of the initial pre-crack and progresses to the two sides. The lamina with 0° – pre-crack is not damaged along the fibre layer, and the fibres still bear the load while the matrix damage extends to the edge of the plate, the lamina is not broken even if the loading process reaches 5000 time-steps.

The tension load-time step curves for eight kinds of lamina are shown in Fig. 15: in the first 2000 steps the laminas are in the elastic phase, and their curves coincide. After the 2000 steps, the curves begin to be gradually different until their maxima are reached. Cracks continue to develop gradually; and after 3400 steps the matrix damage starts to proceed step by step. The damage gradually spreads and eventually leads to fracture, the load-carrying capacity of lamina is decreasing. Generally, the higher the coincidence between the pre-crack and the ply angle, the less the loss of general load-carrying capacity.

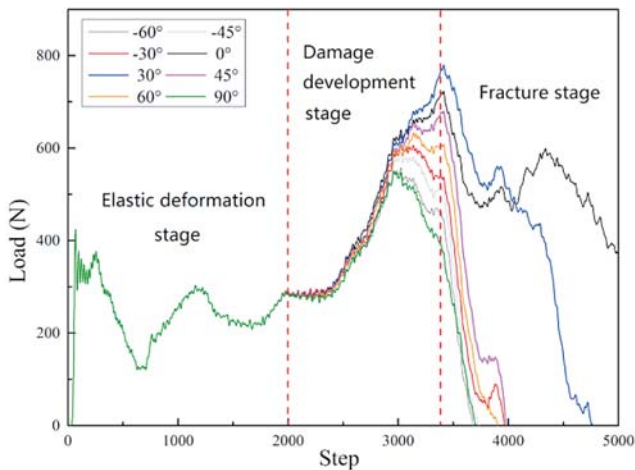


Fig. 15. Tension load-time step curves for laminas with pre-cracks at different angles

DAMAGE ANALYSIS OF COMPOSITE MATERIAL STRUCTURE WITH BOLT CONNECTION

The damage and failure modes of bolted joints under axial load are analyzed by means of the peridynamic method. The model is simplified by omitting the elastic-plastic deformation of bolts. The correction method of displacement is used when the material points in the laminate enter the model of bolted joints at any time [8]; its schematic diagram is shown in Fig. 16.

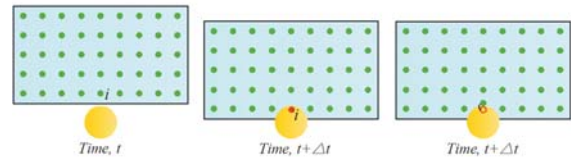


Fig. 16. Schematic diagram of material point relocation

The particulars of composite laminates with bolted joints are: length $L = 90$ mm, width $W = 50$ mm, bolt diameter $\phi = 12$ mm, thickness of laminate plate $t = 8$ mm, the lay-up configuration is $[45/0/-45/90/0]$, the material properties are the same as given in the Tab. 1 above. The PD model of the laminate is generated by 180 material points in length direction and 100 material points in width direction; it means that $\Delta x = 0.5$ mm. The simplified diagram of the bolted joint is shown in Fig. 17.

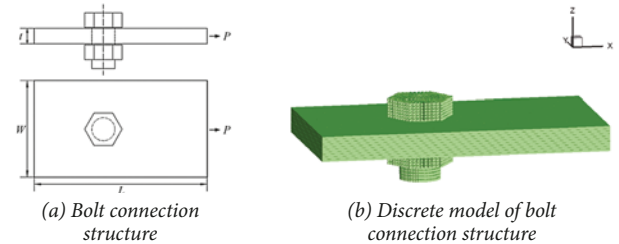


Fig. 17. Simplified bolt connection structure

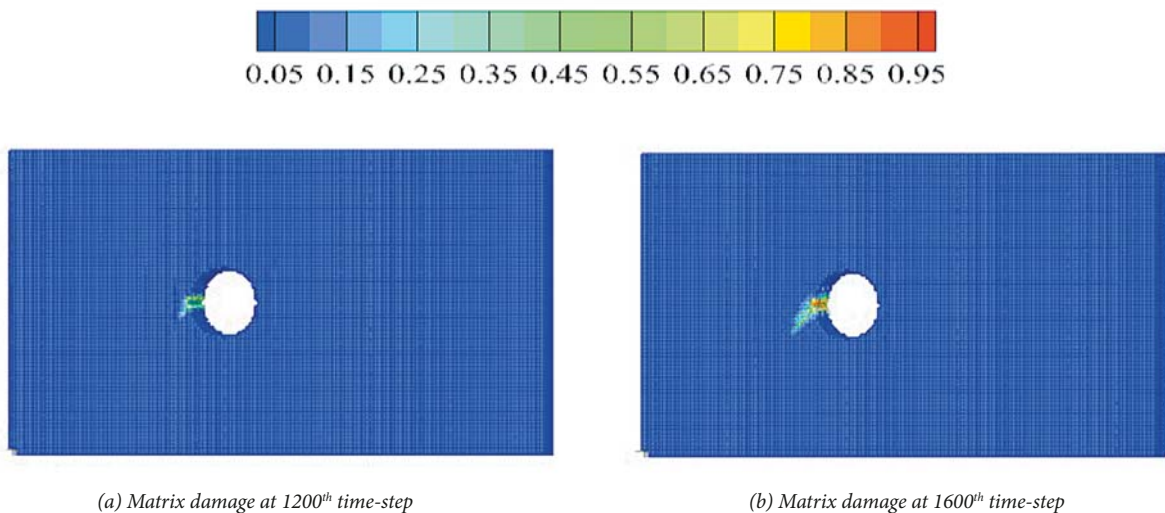
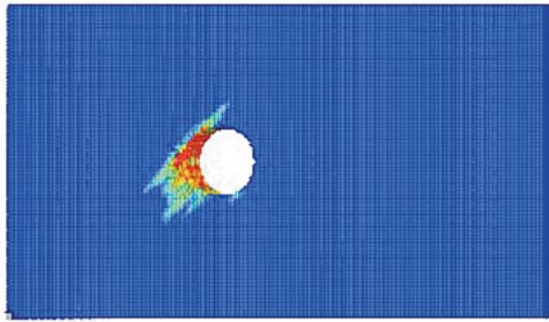
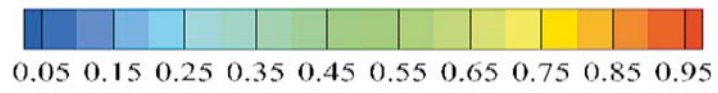
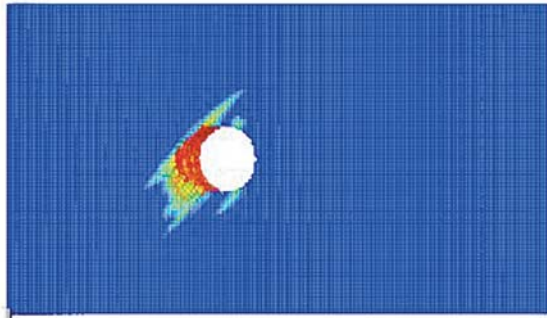


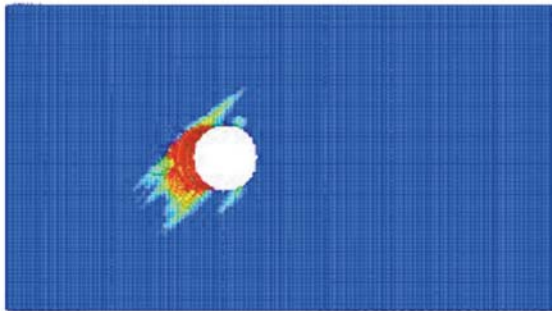
Fig. 18. Results of PD simulation of the bolted joint damage forms and displacements | →



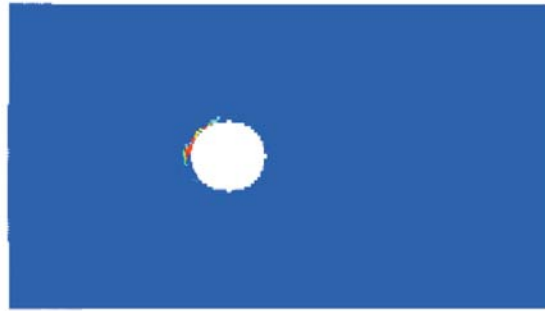
(c) Matrix damage at 4800th time-step



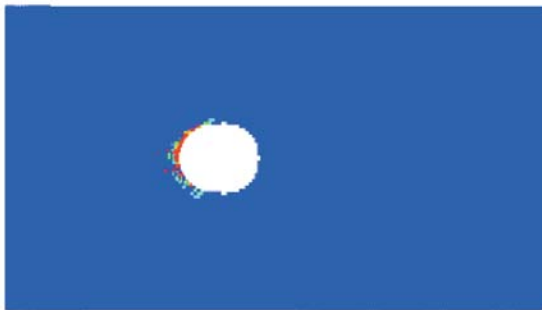
(d) Matrix damage at 6000th time-step



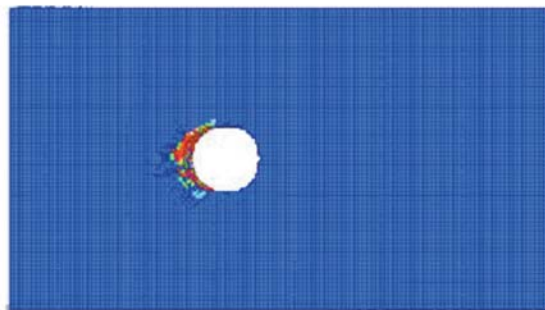
(e) Matrix damage at 12000th time-step



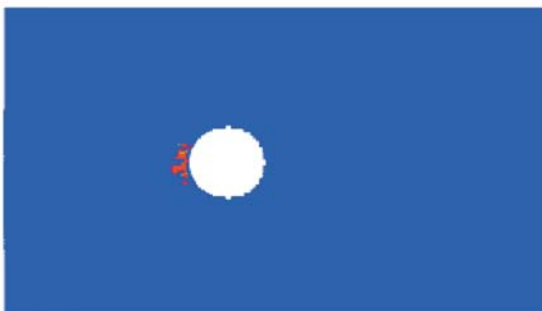
(f) Fibre compression damage at 6000th time-step



(g) Fibre compression damage at 12000th time-step



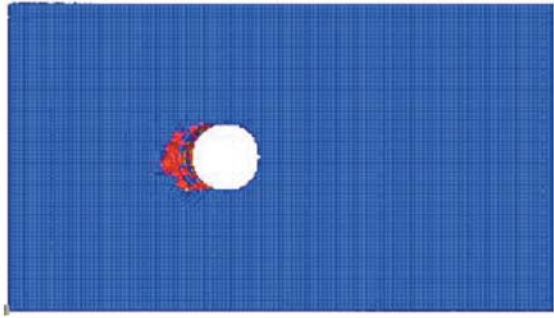
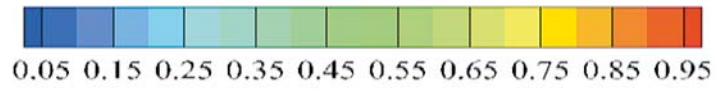
(h) Fibre compression damage at 15000th time-step



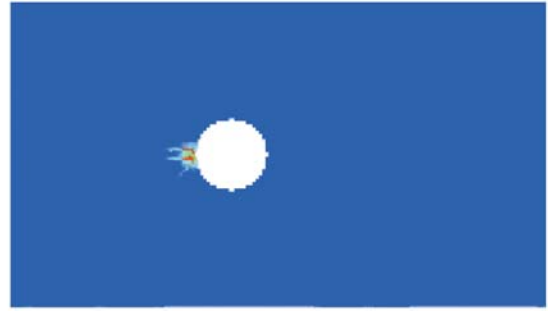
(i) Delamination at 6000th time-step



(j) Delamination at 12000th time-step



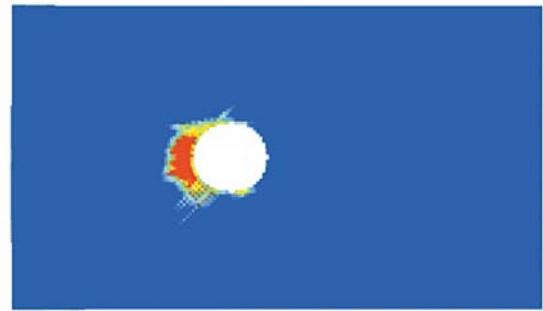
(k) Delamination at 15000th time-step



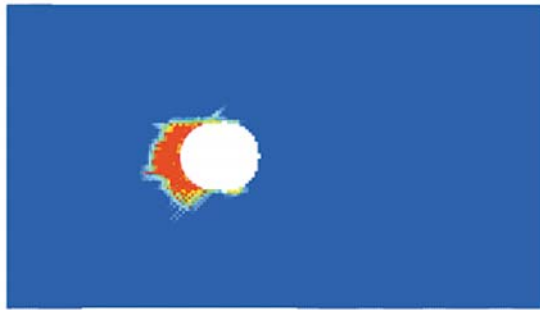
(l) Sheare damage at 16000th time-step



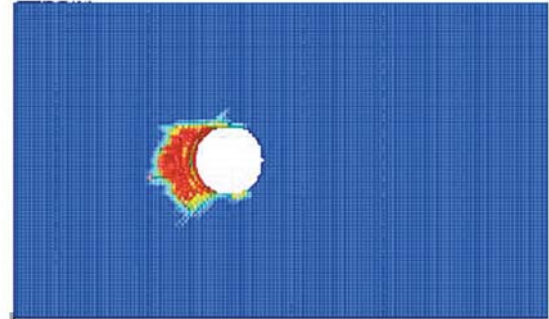
(m) Sheare damage at 4000th time-step



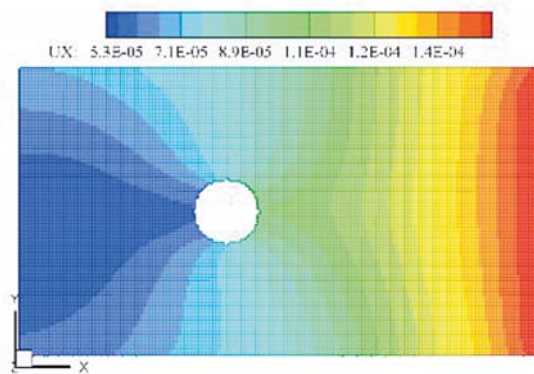
(n) Sheare damage at 6000th time-step



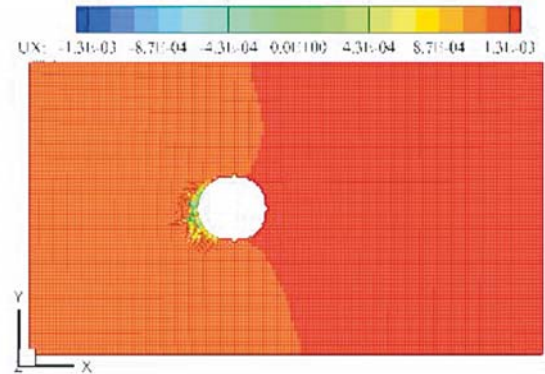
(o) Sheare damage at 12000th time-step



(p) Sheare damage at 15000th time-step



(q) Displacement U_x at 800th time-step



(r) Displacement U_x at 15000th time-step

Fig. 18. Results of PD simulation of the bolted joint damage forms and displacements

The progressive damage results are shown in Fig. 18. Initially, the matrix compression damage occurred around the bolt hole, then, as the load increases, the compression damage is gradually extended to the contact surface of bolt hole. The damage of the matrix is also accompanied by the compression damage of fibres, delamination and shear damage. The damage region is concentrated around the contact zone of the bolt and its hole.

The curve of the extrusion force in function of time – step number for the region of the bolt hole is shown in the Fig. 19. With the increase of the boundary displacement the structure is damaged and its load-carrying capacity decreases. When the load is further increased the bolt hole is crushed, a large damage occurs and the resisting force falls to zero. The force-time step curve correctly reflects the load-carrying characteristics of the composite bolted joints. At the same time, the PD simulation of the bolt connection structure reveals the process of damage occurrence and its expansion without resorting to special crack-growth criteria.

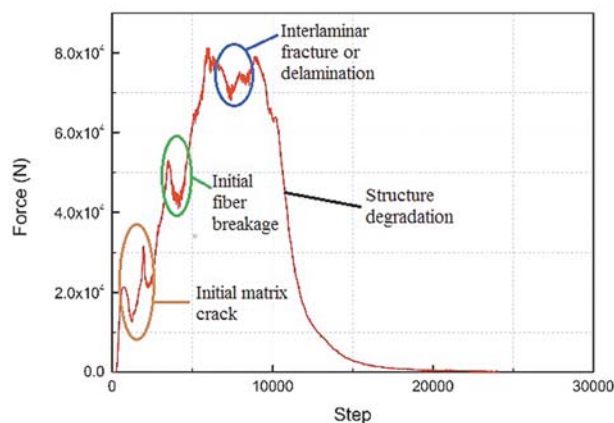


Fig. 19. The force-time step curve for the region of the bolt hole

CONCLUSION

In order to simulate the damage and fracture of fibre reinforced composite laminates and joints, the bond-based peridynamic method suitable for elastic, brittle and anisotropic characteristics of composite material, is used. The bond-based PD model of composites is validated by means of the finite element method and used for analyzing the damage and fracture process of the bolted joints of composite materials under axial load. The mechanism and process of damage occurrence and its expansion revealed that the PD method has a great advantage over the traditional method in the simulation and analysis of damage and fracture. This way it is possible to solve easily the fracture initiation and propagation without resorting to special crack-growth criteria.

ACKNOWLEDGEMENT

The authors would like to acknowledge the support of the National Natural Science Foundation of China (Grant No. 51879048)

REFERENCES

1. Dugdale D.S.: *Yielding of Steel Sheets Containing Slits*. Journal of the Mechanics & Physics of Solids, 1960, 8(2): pp. 100–104.
2. Dolbow J., Belytschko T.: *Numerical Integration of the Galerkin Weak Form in Mesh-free Methods*. Computational Mechanics, 1999, 23(3): pp. 219–230.
3. Silling S.A.: *Reformulation of Elasticity Theory for Discontinuities and Long-range Forces*. Journal of the Mechanics & Physics of Solids, 2000, 48(1): pp. 175–209.
4. Dan Huang, Qin Zhang: *Peridynamic Theory and Its Application*. Advance In Mechanics, 2010, 40(4): pp. 448-459.
5. Madenci E, Oterkus E.: *Peridynamic Theory and Its Applications*. Springer, New York, 2014.
6. Hu Y., Madenci E., Phan N.: *Peridynamic Modeling of Defects in Composites*. 56th AIAA/ASCE/AHS/ASC Structures, Structural Dynamics, and Materials Conference, American Institute of Aeronautics and Astronautics Inc., 2015.
7. Oterkus E., Madenci E.: *Peridynamic Analysis of Fibre-reinforced Composite Materials*. Journal of Mechanics of Materials & Structures, 2012, 7(1): pp. 45–84.
8. Y.L. Hu, Yin Yu, Hai Wang: *Peridynamics for damage analysis method of composite laminates*. Chinese Journal of Theoretical and Applied Mechanics, 2013, 45(4): pp. 624–628.

CONTACT WITH THE AUTHORS

Na-Na Yang

e-mail: nanayang1980@hotmail.com

Tian-You Zhao

e-mail: 894517736@qq.com

Ji-Guang Gu

e-mail: gujiguang@hrbeu.edu.cn

Zhi-Peng Chen

e-mail: henzhipeng2012@163.com

Harbin Engineering University
Nangang, Heilongjiang Province
150001 Harbin
CHINA